JAERI-M
6018

NUMERICAL METHOD TO OBTAIN AN OPTIMUM CONFIGURATION OF EXTERNAL MAGNETIC FIELD COILS IN TOKAMAK DEVICE BY NON-LINEAR PROGRAMMING

February 1975

Kazuo TOI* and Tatsuoki TAKEDA

日本原子力研究所
Japan Atomic Energy Research Institute

JAERI-M 6018

Numerical Method to Obtain the Optimum Configuration of External Magnetic Field Coils in a Tokamak Device by Non-Linear Programming

Kazuo TOI* and Tatsuoki TAKEDA
Nuclear Fusion Lab., Tokai, JAERI

(Received February 7, 1975)

In large tokamak devices in the next phase of fusion research, it seems that equilibrium of the toroidal plasma is maintained essentially by the external control loops and an air-core transformer is used instead of a conventional iron-core transformer. Under this situation the method based on the optimization process using the algorithm of a non-linear programming has been applied in determination of the optimum design of the external magnetic field coils including the control loops for maintaining magnetic field and primary windings of the air-core transformer. It is found that the method is useful for design of the control loops and primary windings in a practical tokamak. The results obtained so far are presented and the procedure of optimization is given in detail and comprehensively.

---

* Present address: Institute of Plasma Physics,
Nagoya University, Nagoya.

JAERI－M 6018

非線型計画法によるトカマク装置の外部磁場コイルの最適配位決定法

日本原子力研究所東海研究所核融合研究室

東井和夫,※竹田辰興

（1975年2月7日受理）

核融合研究の次段階の大型トカマク装置では，トロイダル・プラズマの平衡は本質的に外部制御コイルによって保持されまた空心変流器コイルが広く使われるようになるものと考えられる。このような情況において，平衡保持磁場の為の制御コイル，空心変流器の一次コイル等を含む外部磁場コイルの最適設計の為に，非線型計画法のアルゴリズムを用いた最適化法に基く方法が適用された。現実的なトカマクの制御コイルや一次コイルの設計にあたってこの方法が有効であることが確められた。この報告においては今まで得られた結果が全てまとめられていると共に最適化の手法が詳細にかつ包括的に述べられている。

＊現在　名古屋大学プラズマ研究所

CONTENTS

1. INTRODUCTION

In a conventional tokamak device an equilibrium of a toroidal plasma is maintained by the interactions of the plasma current with its image current in the conducting casing and with the current in several control loops excited by an external power supply. In future large tokamaks with long duration time of the plasma current, however, the contribution of the conducting casing to equilibrium will be considerably reduced because of finiteness of the decay time of the image current. Therefore, the control loops will have an essential role in maintaing the equilibrium of the plasma, although a thin conducting casing may be, still, equipped in the devices from the viewpoint of the stabilization of the fast growing mhd instabilities. Moreover, the primary current for the ohmic heating will be coupled with the plasma current through an air-core transformer in contrast with the conventional iron core transformer. In these cases, the effect of the discreteness of the external magnetic field coils (the control loops and primary windings) which introduces irregularity of the magnetic field over the plasma region becomes more pronounced, e.g., the irregularity causes the possibility of deforming the plasma boundary considerably[1]. Therefore, it is very important to design external magnetic fields carefully.

Some numerical methods are developed to obtain the optimum configuration of the control loops and primary windings, e.g., the virtual casing principle[2,3] and the method based on a linear programming[4]. These procedures determine the value of current in each coil, the position of the coil being fixed beforehand. In these cases the problem is, essentially, reduced to the solution of a linear simultaneous equation because of a linearity of the relation between the current and the magnetic field. As a natural result of the methods we have not any information on the value of current in each coil before solving the equation. Consequently we cannot allocate the magnitude of current in a prescribed value of ratio to each coil, though it is often the case that the ratio of the current is determined beforehand to be, for example, equally distributed among the coils. Moreover by the above methods, the value of current in a certain coil may become, sometimes, extremely large from the practical viewpoint. The following procedure is proposed to overcome the drawbacks of the above-mentioned methods[5]. By the method the optimization of the design of the external magnetic field coils is carried out with respect to the positions and total ampere-turn for the control loops and only the positions for the primary windings, the ratio of current in each coil being fixed at the prescribed value. In the numerical calculation, the non-linear programming has been succesfully applied to the following simplified model.

In the model the positions of the external magnetic field coils are searched on a toroidal surface with a circular cross section to minimize the objective function composed of the sum of the squares of difference between the desired magnetic field and the field due to the coils. In the case of the control loops, for simplicity the expression for the external maintaining magnetic field by Zakharov[6] and Mukhovatov and Shafranov[7] is adopted as the desired magnetic field, that is, the magnetic field is one for the plasma equilibrium with a slight ellipticity and large aspect ratio and it is given on the median plane of the toroidal plasma. Therefore, the objective function to be minimized can be constructed on the median plane, though generally it should be constructed on a toroidal surface which encloses a region of interest, e.g., a plasma surface.

In this article, we devote ourselves to explanation of the practical procedure of the method shown in Ref.5. From above reason some remarks on execution of optimization with constraints, and the flow chart and input data format of the computer code are presented in Appendices A and B, respectively. Section 2 describes the method how to make the objective function for the optimum design of the external magnetic field coil such as control loops and primary windings. In section 3, the procedure of optimum design of control loops and the results are illustratively shown. Problems to be solved concerning the method and the future extension of the method are discussed with some examples in the last section.

2. PROCEDURE FOR THE OPTIMUM DESIGN OF THE EXTERNAL MAGNETIC FIELD COILS

In general the optimum design of the set of the external magnetic field coils is obtained by choosing as an objective function (F) a surface integral of the "length" of the difference vector between the magnetic field produced by the coils and the desired magnetic field and then minimizing the aobve objective function. As the above objective function has, generally, a non-linear dependence on the parameters to be determined, it will be most convenient to use a non-linear programming for the minimization procedure. It is practical and intuitive to choose as the measure of the "length" a square of the Euclidean norm and to represent the integral by a sum of the "length" over J given observation points in the region for the above integration. Thus the objective function to be minimized is derived as,

$$F = \sum_{j=1}^{J} w_j |\mathbf{B}_j - \hat{\mathbf{B}}_j|^2 \qquad (1)$$

where w_j, $\mathbf{B}_j$ and $\hat{\mathbf{B}}_j$ are the weighting coefficient, the vectors of the magnetic flux densities of the magnetic field produced by the coils at the j-th observation point and the desired magnetic field at the same point.

3. OPTIMUM DESIGN OF THE CONTROL LOOPS

(3-1) THE OBJECTIVE FUNCTION AND INTRODUCTION OF CONSTRAINTS

In this subsection, we discuss the procedure for the optimum design of the control loops in a tokamak device. In subsections 3-2 and 3-3, the results of calculation for a practical device are shown with some illustrations. It should be remarked that as shown in the last section the generalization of the procedure of this section is straightforward. As mentioned in the introduction, the observation points are chosen on the median plane of the toroidal plasma in the model of this section. Therefore, Eq.(1) is reduced to the simpler expression as,

$$F = \sum_{j=1}^{J} w_j (B_{\perp j} - \hat{B}_{\perp j})^2 \qquad (2)$$

where $B_{\perp j}$ and $\hat{B}_{\perp j}$ are the vertical components of the above-mentioned magnetic fields at the median plane. Here we restrict during the course of iterations the motion of the 2M control loops on a toroidal surface with a circular cross section (M loops on the upper half surface and M loops on the lower half surface at the mirror images of the upper loos) as shown in Fig.1. The restriction greatly simplifies the expression of the objective function because in this case the position of i-th control loop is represented by only one parameter, θ_i. It is not, however, the essential restriction on the problem and can be removed if necessary. The current in the i-th control loop is represented as $\alpha_i I$,

where $\alpha_i I$, is the prescribed ratio of current in the i-th control loop ($\sum_{i=1}^{M} \alpha_i = 0$) and I is the total ampere-turn divided by $\sum_{i=1}^{M} |\alpha_i|$. Thus, the objective function F for the system of 2M control loops is expressed by (M + 1) variables, that is, the M poloidal angles, θ_i's (i=1, 2, ···, M) and the normalized ampere-turn I. As the number of the observation points (J) should be sufficiently larger than that of the unknown parameters (M + 1), about 7M observation points have been prepared through all the calculations presented in the paper. As the computer code for the minimization, we used the non-linear programming code published by Van der Voort and Dorpema[8]. In the code the minimization of the objective function is carried out by one of three methods, that is, the gradient method, the modified Newton Raphson method and the Newton Raphson method depending on the property of the Hessian matrix of the objective function. For the clear demonstration of the applicability of the method to the problem, the following two quantities, the local and mean deviations of the designed magnetic field from the desired one, are defined as,

$$\Delta B_\perp(R_j)/\hat{B}_\perp(R_j) \equiv [B_\perp(R_j) - \hat{B}_\perp(R_j)]/\hat{B}_\perp(R_j) \tag{3}$$

$$\delta B_\perp/\hat{B}_{\perp o} \equiv [\{\sum_{j=1}^{J} [B_\perp(R_j) - \hat{B}_\perp(R_j)]^2\}/(J - 1)]^{1/2}/\hat{B}_{\perp o} \tag{4}$$

where it should be remarked that the position of the j-th observation point is $R = R_j$ and $Z = 0$ and $\hat{B}_{\perp o}$ denotes the value of the desired magnetic field on plasma axis. In the problem of this kind, where the magnetic field is optimized on the median plane, the spatial variation of the decay index ($n = -(R/B_\perp)\cdot(dB_\perp/dR)\,|_{Z=0}$) is also one of the stringent measures of fitness of the optimized magnetic field. In the subsequent subsections we examine the above three parameters, i.e., $\Delta B_\perp(R_j)/\hat{B}_\perp(R_j)$, $\delta B_\perp/\hat{B}_{\perp o}$ and n, to investigate the applicability of the method to the optimum design of the control loops.

Basically the optimum design of the control loops can be obtained by minimizing the above objective function. In the course of analyses of this paper, however, the optimum positions and ampere-turn of the control loops have been obtained straightforwardly only when M is small ($M < 6$). When M is large ($M \geq 6$), the above-mentioned procedure meets a difficulty, that is, the convergence of the solution is remarkably deteriorated. It is found that the deterioration of the convergence results from the repeating exchanges of the positions among adjacent control loops. The difficulty is, therefore, overcome by introducing appropriate constraints which forbid the exchange of the positions of the control loops. The constraints are expressed, in this case, as,

$$g_1 = \theta_1 - \theta_{min} > 0$$

$$g_i = \theta_i - \theta_{i-1} > 0 \quad (i=2,3,\cdots,M) \tag{5}$$

$$g_{M+1} = \theta_{max} - \theta_M > 0$$

where the first and last conditions are introduced so that all control loops exist in a region between θ_{min} and θ_{max}. It should be noted that such constraints as g_1 and g_{M+1} are introduced for arbitrarily chosen groups of control loops and forbidden regions for the control loops can be provided at any region on the toroidal surface. We solved the constrained minimization problem by "Sequential Unconstrained Minimization Technique" (SUMT)[9], introducing a penalty function P and transforming the objective function F with above constraints into the objective function without the constraints $\tilde{F}$, as,

$$\tilde{F}(\theta_1,\theta_2,\cdots,\theta_M, I; \gamma_s)$$

$$= F(\theta_1,\theta_2,\cdots,\theta_M, I) + P(\theta_1,\theta_2,\cdots,\theta_M; \gamma_s) \tag{6}$$

where the penalty function is expressed as,

$$P(\theta_1,\theta_2,\cdots,\theta_M; \gamma_s) = \gamma_s \sum_{i=1}^{M+1} \frac{1}{(g_i)^K} \tag{7}$$

where K is the given positive integer and γ_s is the perturbing parameter which is decreased in a prescribed manner as the values of the variables approach the optimum ones. Practically the modified objective function $\tilde{F}$ is minimized for a fixed value of γ_s by using the above-mentioned computer code. After the minimum of $\tilde{F}$ is searched within the prescribed accuracy, the perturbing parameter is reduced by a decreasing rate $\hat{\gamma}$ and the minimization of $\tilde{F}$ is carried out again for the new parameter $\gamma_{s+1} = \gamma_s \cdot \hat{\gamma}$. In Appendix A, some remarks on execution of optimization with constraints are shown.

(3-2) MAGNETIC FIELD PRODUCED BY LINE CURRENTS ON A CYLINDRICAL SURFACE

For the examination of the convergence of the solution and the deviation of the designed magnetic field produced by the control loops from the desired one after the above optimization, a set of "control loops" composed of line currents on a cylindrical surface which produces a uniform vertical magnetic field inside the cylinder is designed by the method described in the previous subsection. The calculations are carried out for the following parameters; the radii of the cylinder on which the line current exist and the cylindrical plasma are r_s = 0.5 m and a_p = 0.4 m, respectively, and the observation points of the magnetic field are chosen

on a diameter of the plasma.

First, the objective function F without the penalty terms has been minimized. As stated in the previous subsection, in the cases of large M ($M \geq 6$), the solution has not converged on the optimum point but oscillates around a certain point. As the result of the phenomenon, the mean deviation of the field from the desired uniform magnetic field also oscillates and is not lowered below a certain value. An example of the results is shown by a cross in Fig.2 for the case of M = 8. In the next place as it is known that the phenomenon results from the repeating exchanges of the control loops, the constraints (Eq.(5)) is introduced and modified objective function $\hat{F}$ is minimized. In this case, however, the "forbidden region" is not set up, i.e., $\theta_{min} = 0$ and $\theta_{max} = \pi$. By introducing the constraints and choosing the perturbing parameters appropriately, the exchanges of the control loops are suppressed completely and the convergence of the solution was attained favourably. Figure 2 shows the mean deviation of the designed magnetic field from the desired one for the cases of M = 2, 4, 6, 12, and 16. Among them , the solution for M = 16 did not converge on the optimum point due to the truncation and cancellation errors though the calculations were executed in double precision. It is seen, however, from the figure that the deviation of the designed magnetic field from the desired one is small enough for a practical problems.

For the case of M = 12, the optimum positions of the control loops and the deviation of the designed magnetic field at the observation points on the diameter of the plasma (Eq.(3)) are shown in Fig.3. Figure 4 is the magnetic lines of force for the same case, where the slight asymmetry of the pattern of the field lines is due to the fact that the field calculation for the plotting is carried out not for a strictly cylindrical case but for the very thin toroidal case ($R_o/r_s = 100$). It is very useful to know how much extent the designed magnetic field is deviated from the uniform magnetic field at the region except the diameter where the observation points are located, because there remains a possibility that the magnetic field is distorted considerably at the region except the diameter as expected when the solution of the problem is obtained by solving a differential or integral equation. One of measures for the examination of the possibility is to plot the magnetic lines of force as seen in Fig.4 and another is to plot the following two-dimensional pattern of the deviation over the region of interest. In the case of uniform field the deviation of the designed magnetic field from the desired one is expressed as,

$$\varepsilon \equiv \frac{|\mathbf{B} - \mathbf{B}_o|}{|\mathbf{B}_o|} = \sqrt{(B_X/\hat{B}_{\perp o})^2 + [(B_Z - \hat{B}_{\perp o})/\hat{B}_{\perp o}]^2} \qquad (8)$$

$$\mathbf{B} = (B_X,\ 0,\ B_Z)$$

$$\mathbf{B} = (0,\ 0,\ \hat{B}_{\perp o})$$

where $\mathbf{B}$ and $\mathbf{B}_o$ are the vectors of the magnetic flux densities of the designed magnetic field and desired uniform magnetic field, respectively. In Fig.5, the constant ε lines (ε = 1.0 %) are shown for the various values of the mean field deviation (Eq.(4)) and it is seen that the region where the deviation is less than 1.0 % spreads considerably with decreasing the mean field deviation at the observation points on the diameter.

(3-3) OPTIMUM CONFIGURATION OF CONTROL LOOPS IN A PRACTICAL TOKAMAK DEVICE

In this subsection, we describe the design of the control loops in a practical tokamak device in some detail. Strictly speaking, the maintaining magnetic field required for the equilibration of the tokamak plasma should be optimized over the whole plasma surface of the toroidal plasma as stated in the introduction. For tokamak plasma with the slight ellipticity, large aspect ratio and uniform current density, however, the required maintaining magnetic field is well represented by the values on the median plane of the toroidal plasma[6,7]. The maintaining magnetic field on the median plane is expressed as,

$$\hat{B}_{\perp} = \hat{B}_{\perp o}[1.0 - \frac{R - R_p}{R_p} n_o] \tag{9}$$

where

$$\hat{B}_{\perp o} = \frac{\mu_o I_p}{4\pi R_p} [\ell n(8R_p/a_p) + \beta_I - \frac{5}{4}]$$

$$n_o = \frac{\frac{3}{4} \ell n(8R_p/a_p) - \frac{17}{16} + (1.0 - \ell_Z/\ell_R)R_p^2/a_p^2}{\ell n(8R_p/a_p) + \beta_I - \frac{5}{4}}$$

and I_p, β_I, R_p, a_p, ℓ_Z, ℓ_R, R and μ_o are the plasma current, the ratio of the gas-kinetic pressure to the poloidal magnetic pressure, the major and mean minor radii of the plasma , the vertical and horizontal semi-axes of the ellipse, the distance of the observation position from a symmetric axis of the plasma and the permeability of the vacuum, respectively. The decay index of the magnetic field on the plasma axis is denoted by n_o. It should be also noted that Eq.(9) is valid over the whole plasma region up to the first order of the inverse aspect ratio[6] and, therefore, the radial component of the maintaining magnetic field is expressed as,

$$B_R = -\hat{B}_{\perp o} \cdot n_o \frac{Z}{R_p} . \tag{10}$$

The optimum design of the control loops are obtained for a large tokamak with the following parameters; R_o = 3.05 m, r_s = 1.25 m, R_p = 3.00 m, a_p = 1.00 m, $\ell_Z = \ell_R$ and β_I = 1.0. In the calculation, the modified objective function ($\tilde{F}$) is minimized and two different cases with and without forbidden region are investigated. The mean deviation of the designed magnetic field (Eq.(4)) for the case without forbidden region is about the same as the results for the cylindrical case shown in Fig.2. The mean deviation for the case with forbidden region is, however, much more larger than for the above case. The deviation reasonably increases with increasing extent of the forbidden region. In the followings the results for the cases of M = 4, 8 and 12 are shown with some illustrations. Figures 6-(a), (b), (c) and (d) show the optimum positions of the control loops and the deviation of the designed magnetic field from the desired one (Eq.(3)) for various values of M and α_i's. The profiles of the magnetic fields and decay indices are also shown for the case of M = 12. The two-dimensional patterns of the magnetic lines of force corresponding to Figs.6-(a), (b), (c) and (d) are shown in Figs.7-(a), (b), (c) and (d), respectively. From the variations of the radial and vertical components of the magnetic field along the radial and vertical directions, it is seen that the designed magnetic field has the distribution given by Eqs.(9) and (10) over almost whole plasma cross section, though the optimization of the magnetic field is carried out only on the median plane of

the toroidal plasma. Figures 8 and 9 show those of the case with forbidden regions near $\theta = 0$ and $\theta = \pi$ corresponding to Figs.6-(c) and 7-(c). In Appendix B, the flow chart of the above optimization calculation and the input data format of the code are presented for users of the code.

The results thus obtained can be compared with those with continuous surface current distribution in a conducting casing located at the toroidal surface on which the control loops move by Fourier-analyzing the discretized current distribution. Figure 10 shows the distributions of the surface current obtained by summing the Fourier components to the sixth harmonics for Fig.3 and Fig.6-(c).

4. DISCUSSION

It is shown in the previous sections that the procedure based on the non-linear programming is successfully applied to the determination of the optimum configuration of the control loops which produce the maintaining magnetic field in a tokamak device. Though in this article the applicability of the method to the optimization of the maintaining magnetic field is investigated under several restrictions, this procedure is straightforwardly applied to more general problems without such restrictions.

For example, the "direct equilibrium problem"[2]* of a tokamak plasma which has not a conducting casing but a set of control loops can be solved without approximation by the above optimization procedure in conjunction with the virtual casing principle[2,3]as follows. Firstly,the distribution of the maintaining magnetic field on a plasma surface is

---

* In general an mhd equilibrium of an axisymmetric toroidal plasma is expressed by a non-linear differential equation of the flux function of the poloidal magnetic field where the distribution of the toroidal current density is an arbitrary given function. The problem of determing the vacuum field outside the plasma on the basis of the flux function which is obtained by solving the non-linear differential equation for a fixed boundary plasma is called the "direct equilibrium problem" in Ref.2.

obtained by the virtual casing principle. Then the parameters concerning the control loops is determined so that the magnetic field produced by the control loops should be bestfit for the magnetic field. We show schematically the above procedure for the optimum design of control loops in Fig.11 comparing with the method in Ref.2. Determination of the optimum configuration of primary windings is another example of the application of the method. As all the windings are conected in series in the case of primary windings, the ratio of the current allocated to each coil must be determined before the optimization. Therefore, the optimizations with respect to the positions of the windings by fixing the current in each winding are more desirable than those with respect to the current in each winding by fixing the positions and total ampere-turn of the windings. Generally speaking, in designing primary windings the magnetic field by the windings in the plasma region should be reduced as low as possible, while the necessary induced electric field at the plasma is kept constant. In the practical case, however, the space where the primary windings can move during the optimization procedure is restricted to a comparatively small region and the coupling constant of the primary windings to the plasma does not vary considerably. Therefore, we can obtain an

optimum design of the primary windings, minimizing the total magnetic energy integrated over the cross section of the plasma and keeping the total ampere-turn of the windings constant. Preliminary calculations concerning the optimum design of the primary windings are also carried out where the magnetic energy is minimized on the surface of the toroidal plasma. Figure 12 shows an example of the optimum positions of the primary windings, the two-dimensional pattern of the magnetic lines of force and the magnitude of the magnetic field (gauss) for the total ampere-turn of 1 MAT.

In applying the method to the above problems, however, two points should be remarked. Firstly the number of calculation of the magnetic field for one evaluation of the objective function is $M \times J$ times, where J is chosen to be several times of M, and for the one iteration of the optimization the objective function is estimated at least by the number of variables of the objective function. Therefore, the computation time for the optimization of the system of 2M coils is proportional to more than third power of M and the optimization will be considerably difficult with increasing M. But in the case of the control loops, for example, M of more than 20 will not be required from the technical point of view at least when there is no "forbidden region". Even when more control loops are required, however, we can reduce the computation time, for example, by dividing the unknown parameters into two

groups and minimizing the objective function alternatively with respect to the two groups of the parameters. Secondly as the expression of the derivatives of the objective function becomes extremely complicated for the case where the observation points of the magnetic field are not restricted only on the median plane, the computer code of the non-linear programming where the derivatives of the objective function are not required is desirable. For this purpose, "the conjugate gradient procedure without calculating derivatives" by Powell[10] or "the simplex method" by Nelder and Mead[11] will be more easily applied, because of the simplicity of formulation of the problem. The simplex method is applied to obtain the above-mentioned example on the optimization of the primary windings because the derivatives of the objective function are too complicated due to the fact that the observation points of the magnetic field are not on the median plane. Generally speaking, the fewer numbers of iterations are required for convergence by a non-linear programming code which uses the derivatives of the objective function. In this case, however, the computation time for one iteration is very large for a problem with complicated derivatives of the objective function. Therefore, it depends greatly on the problem to be solved, which kind of the computer code is desirable.

ACKNOWLEDGMENT

The authors wish to express their sincere thanks to Drs. S. Tamura and T. Kobayashi for stimulating discussions on this subject. Drs. M. Tanaka and M. Yoshikawa are acknowledged for the continuing interests in the problem and the encouragements. They are also grateful to Dr. S. Mori for the continuing encouragement.

APPENDIX A. REMARKS ON EXECUTION OF OPTIMIZATION WITH CONSTRAINTS

The optimization problem with constraints is solved by appropriate transformations. Two different transformations are used, i.e., the method in which the variables to be determined are transformed into new ones [12] and the other where the objective function is modified. The latter is still divided into the following two kinds of methods. One is the method where the penalty function corresponding to the constraints is added to the unconstrained objective function and the modified objective function without constraints is minimized as shown in subsection 3.1 (SUMT) [9] and the other is the method in which the objective function is modified to take a large positive value over the whole forbidden region, which is especially effective in the case of the minimization by the simplex method [11].

We carried out the optimum design of control loops by the SUMT method. In this method, it is very important to choose properly the initial value of the perturbing parameter γ_1 and the decreasing rate $\hat{\gamma}$. We choose γ_1 so that the value of the penalty function P is about ten to hundred times as large as the value of the original objective function F. When the minimum of the modified objective function $\tilde{F}$ is searched within the prescribed accuracy, the perturbing parameter is reduced by a decreasing rate $\hat{\gamma}$. For $\hat{\gamma}$ = 0.1 - 0.5, the desirable

results are obtained. If $\hat{\gamma} \lesssim 0.05$, the constraints have been violated in the course of iterations. Fig.13 shows the behaviour of the ratio of the penalty function to the original objective function (P/F) as a function of the number of iterations for $\hat{\gamma}$ =0.1 and 0.05. In the case of $\hat{\gamma} = 0.05$, the constraints are violated at 28th iteration. On the other hand, as seen from the figure for $\hat{\gamma} = 0.1$, when the solution converges the optimum value of the original objective function, P/F is almost constant for a certain perturbing parameter γ_s and decreases at the rate of $\hat{\gamma}$ (ITR $\gtrsim$ 250).

It should be remarked that the simplex method is effective for the optimization problem with constraints from reason that the introduction of the constraints is very easy.

APPENDIX B. FLOW CHART AND INPUT DATA FORMAT OF FORTRAN PROGRAM FOR OPTIMUM DESIGN OF CONTROL LOOPS

B-1. Flow Chart

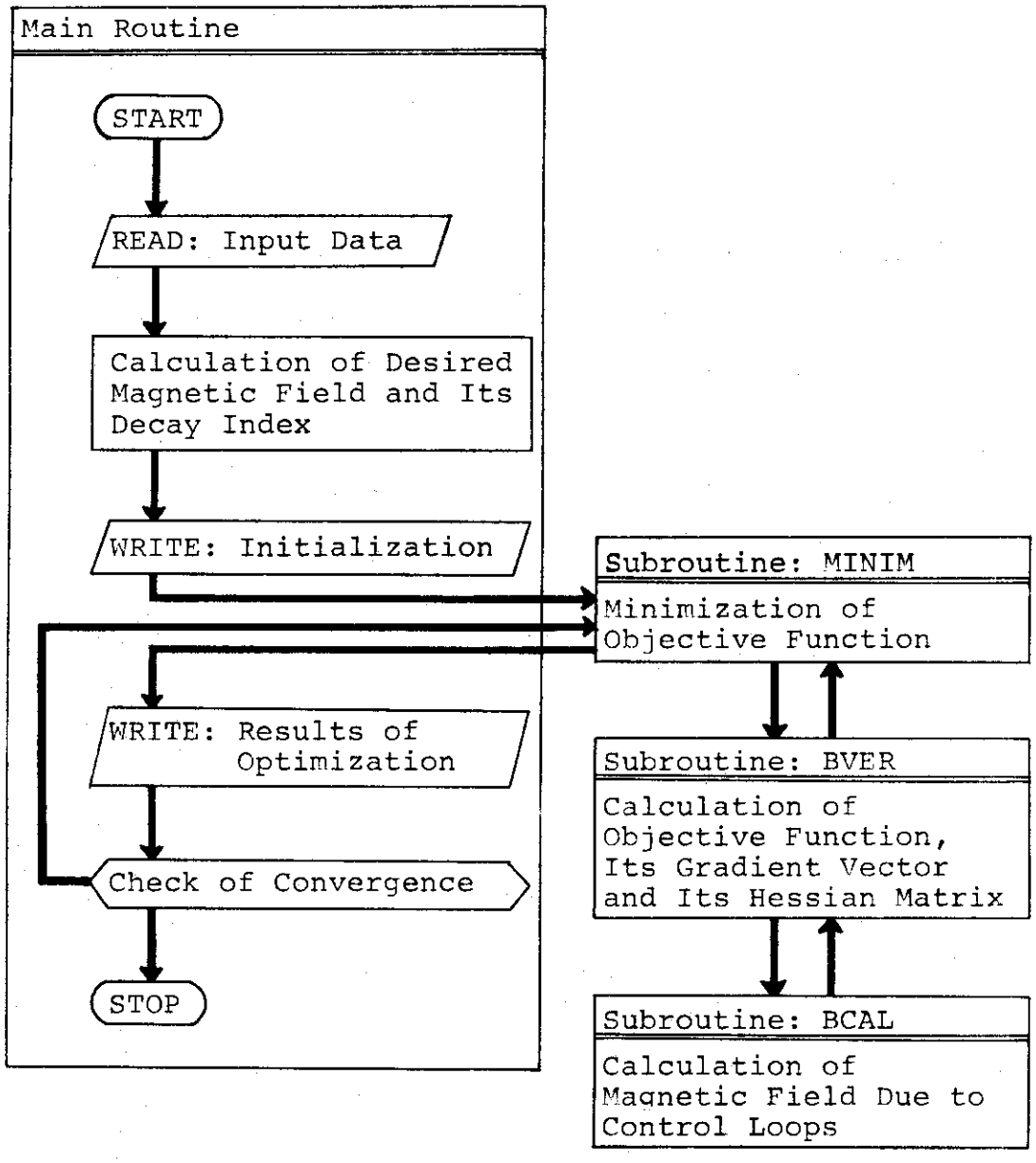

B-2. Input Data Format

Card 1.

M	J	(2)	(0)	INITG[1)]	(0)	K[2)]	(0)	KAFC[3)]
I6	I6	I6	I6	I6	I6	I6	I6	I6

Card 2.

ISIGM[4)]	IPUNCH[5)]
I6	I6

Card 3. Plasma Parameters

R_o(m)	r_s(m)	R_p(m)	a_p(m)	β_I	$\hat{B}_{\perp o}$(Wb/m^2)
F6.3	F6.3	F6.3	F6.3	F12.4	E12.4

Card 4. Both Ends of Observing Region

R_{min}(m)	R_{max}(m)
F6.3	F6.3

Card 5. Forbidden Region

θ_{min}(rad.)	θ_{max}(rad.)
E12.5	E12.5

Card 6.

ISIGM=0

α_1	α_M
F6.1	F6.1

ISIGM≠0

α_i; i=1,...,M
12F6.1

Card 7. Initial Guess for Optimization

INITG=0

θ_1(rad.)	θ_M(rad.)
E12.5	E12.5

INITG≠0

θ_i(rad.); i=1,...,M
6E12.5

Card 8. Initial Guess for Optimization

I (A)
E12.5

Card 9.[6)]

ε_X	ε_F	ε_G	IMAX	NIT
E12.5	E12.5	E12.5	I3	I3

Card 10. Initial Value of Perturbing Parameter

γ_1
E12.5

Card 11. Decreasing Rate

$\hat{\gamma}$
E12.5

Card 12.

ε 7)
E12.5

---

1) INITG=0 or ≠0

2) Positive integer (In this calculation: K=2).

3) Fourier components are calculated to the KAFC-th term.

4) If ISIGM=0, then $|\alpha_i|=|\alpha_{i+1}|$, i=1, 2, ..., M-1.
If ISIGM≠0, then α_i is given arbitrarily ($\sum_{i=1}^{M} \alpha_i=0$).

5) If IPUNCH≠0, then the results in the course of optimization (corresponding to Cards 7, 8, 9, 10 and 11) are punched out.

6) Prescribed accuracies (ε_X, ε_F and ε_G), the maximum number of iteration (IMAX) and gradient method (NIT) in the minimization subroutine MINIM.

7) If P/F (P: penalty function, F: original objective function without constraints) is less than or equal to ε, then the optimization calculation is stopped.

REFERENCES

[1] YOSHIKAWA, S., Phys. Fluids 15 (1972) 1683.

[2] ZAKHAROV, L. E., Nucl. Fusion 13 (1973) 595.

[3] SHAFRANOV, V. D., ZAKHAROV, L. E., Nucl. Fusion 12 (1972) 599.

[4] KOBAYASHI, T., TAMURA, S., TANI, K., JAERI-M 5898 (1974) (in Japanese).

[5] TOI, K., TAKEDA, T., submitted to Nucl. Fusion.

[6] ZAKHAROV, L. E., Soviet Phys. Tech. Phys. 16 (1971) 645.

[7] MUKHOVATOV, V. S., SHAFRANOV, V. D., Nucl. Fusion 11 (1971) 605.

[8] VAN DER VOORT, E., DORPEMA, B., Report of the Joint Nuclear Research Center, EUR 4777 e (1972).

[9] FLACCO, A. V., MACCORMICK, G. P., Nonlinear Programming: Sequential Unconstrained Minimization Techniques, John Wiley (1968).

[10] POWELL, M. J. D., The Computer Journal 7 (1964) 155.

[11] NELDER, J. A., MEAD, R., The Computer Journal 7 (1965) 308.

[12] BOX, M. J., The Computer Journal 9 (1966) 67.

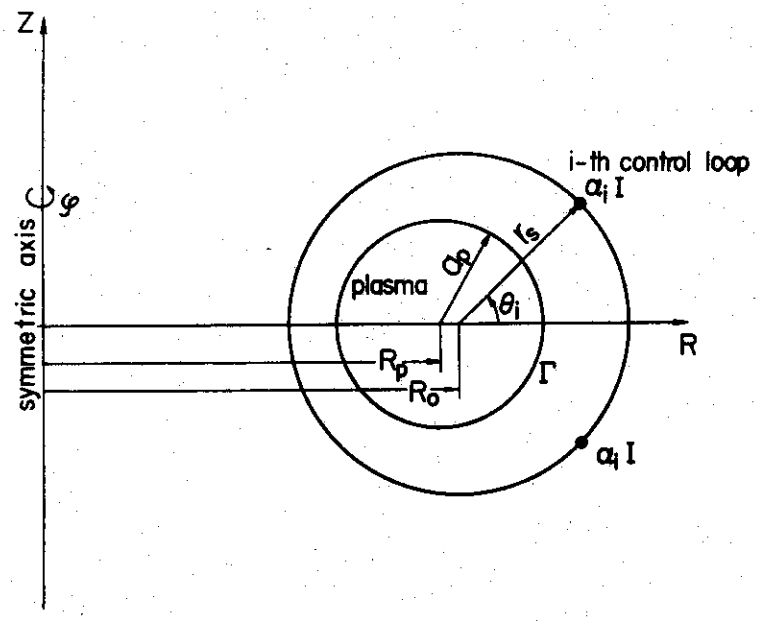

Fig.1. Geometry of the control loops. (R, φ, Z) is the cylindrical coordinate. The control loops are put on the toroidal surface with a major and minor radii R_o and r_s, respectively. The i-th control loop current is $\alpha_i I$ and the total ampere-turn is $\sum_{i=1}^{M} |\alpha_i| I$. Γ designates a plasma surface.

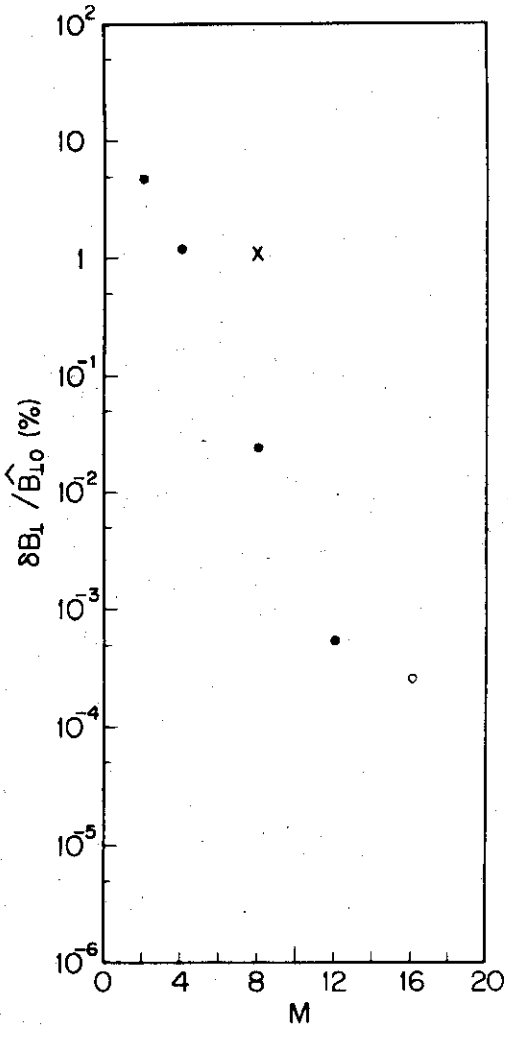

Fig.2. Dependence of the mean deviation of the designed magnetic field from the desired one (Eq.(4)) on M in the cylindrical case, where the total number of control loops are 2M. The deviation of the magnetic field for the case of M = 16 (open circle) is larger than that expected from extrapolation of the results of M < 16 (solid circle) because of the truncation and cancellation errors.

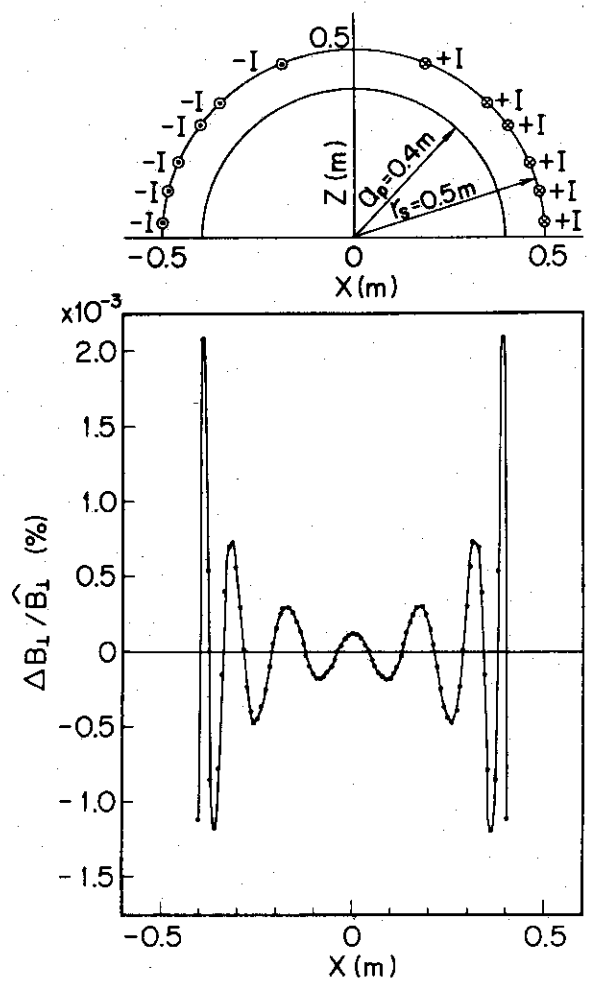

Fig.3. The optimum positions of the control loops (M = 12) and the distribution of the deviation of the designed magnetic field from the desired one on the diameter of the plasma (Eq.(3)), where I= 0.131579 MA for $\hat{B}_{\perp o}$ = 1.0 Wb/m^2.

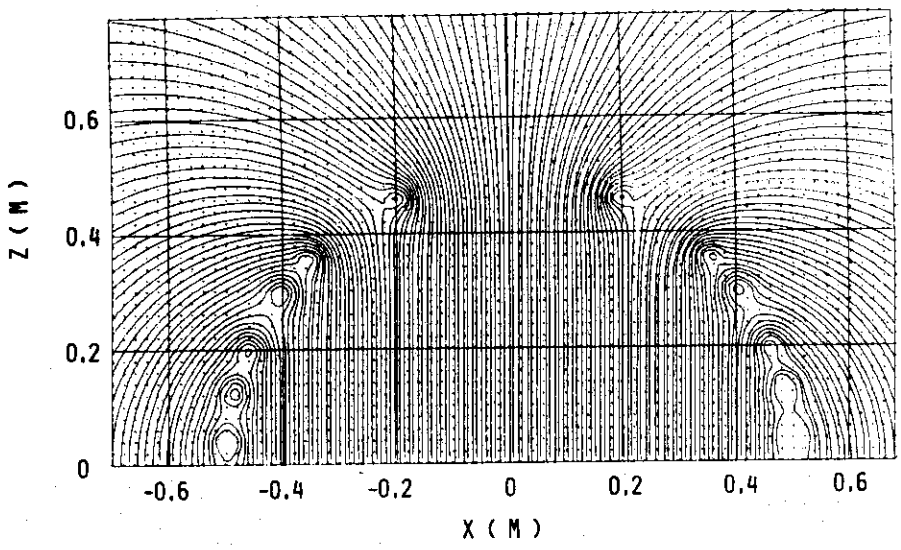

Fig.4. Two-dimensional pattern of the magnetic lines of force for the case shown in Fig.3.

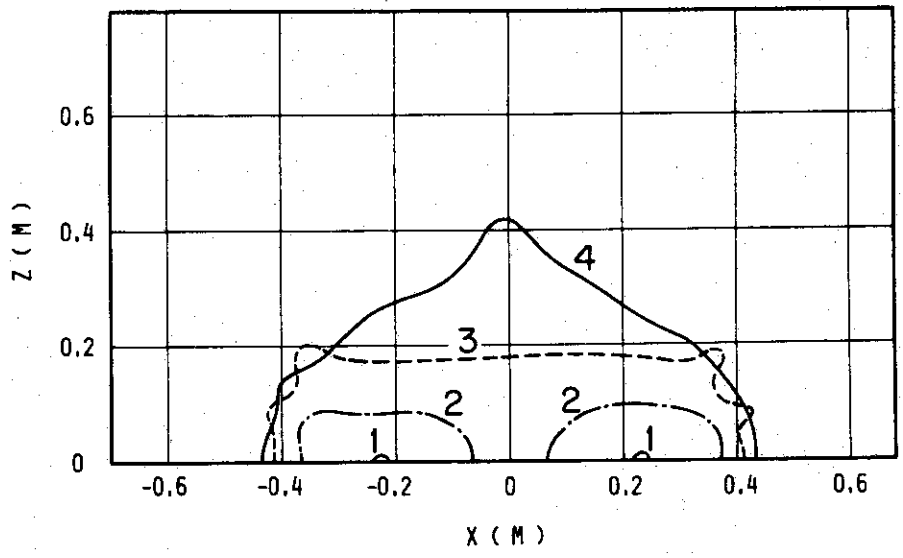

Fig.5. Constant ε lines (ε = 1.0 %) obtained in the course of the iterations of the optimization for the various mean deviations of the designed magnetic field (Eq.(4)); 1. $\delta B_{\perp}/\hat{B}_{\perp o}$ = 9.3 %, 2. $\delta B_{\perp}/\hat{B}_{\perp o}$ = 0.85 %, 3. $\delta B_{\perp}/\hat{B}_{\perp o}$ = 0.10 %, 4. $\delta B_{\perp}/\hat{B}_{\perp o} = 5.5 \times 10^{-4}$ % (converged result shown in Figs.3 and 4).

Fig.6. The optimum positions of the control loops in the toroidal case. The distributions of the deviation of the designed magnetic field from the desired one (Eq.(3)) are shown for M=4, 8 and 12. For M=12, the designed maintaining magnetic field and the decay index are also shown by the dots, and the desired distributions are shown by the broken lines.

(a) M = 4, where I = 1.03022 MA for $\hat{B}_{\perp o}$ = 1.0 Wb/m^2

(b) M = 8, where I = 0.53102 MA for $\hat{B}_{\perp o}$ = 1.0 Wb/m^2

(c) M = 12 (α_i = 1.0 (i=1, 2, ..., 6), α_i = -1.0 (i=7, 8, ..., 12)), where I = 0.356456 MA for $\hat{B}_{\perp o}$ = 1.0 Wb/m^2

(d) M = 12 (α_1 = 3.0, α_2 = α_3 = 2.0, α_4 = α_5 = α_6 = 1.0, α_7 = α_8 = α_9 = -1.0, α_{10} = α_{11} = -2.0, α_{12} = -3.0), where I = 0.206639 MA for $\hat{B}_{\perp o}$ = 1.0 Wb/m^2.

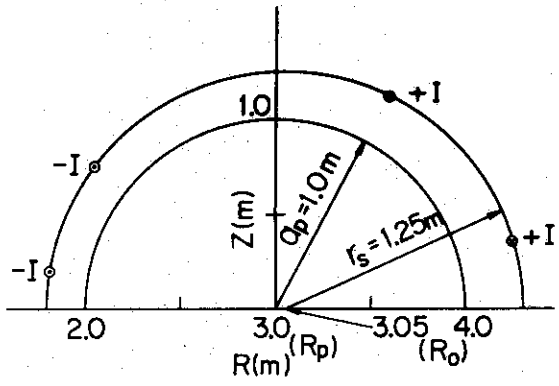

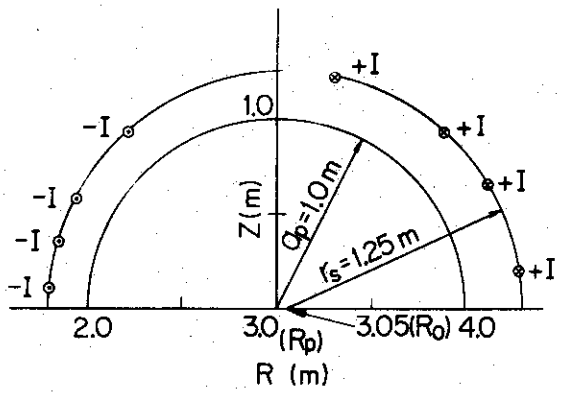

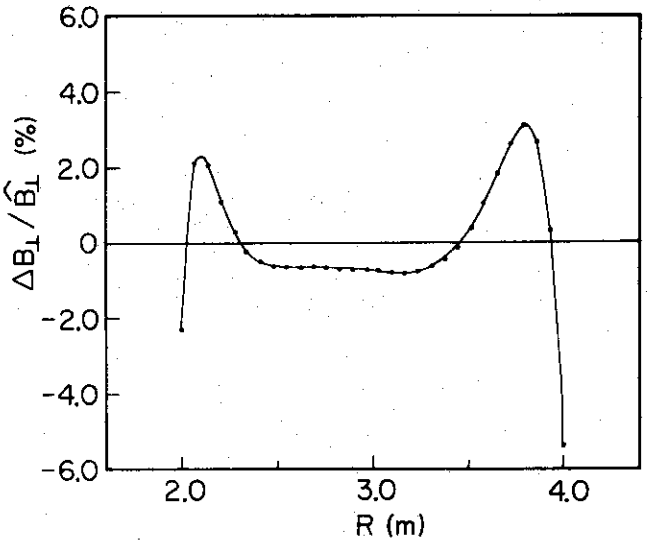

(a)

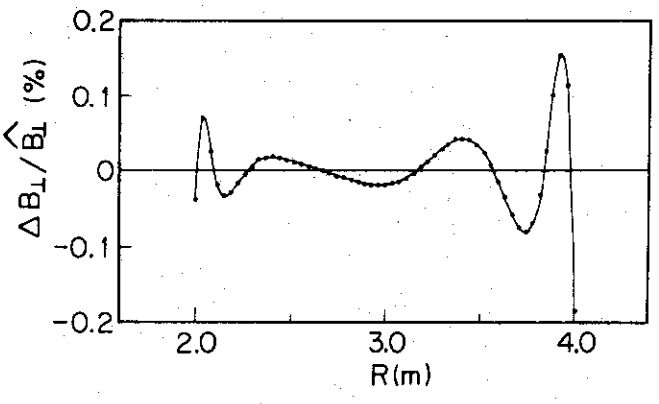

(b)

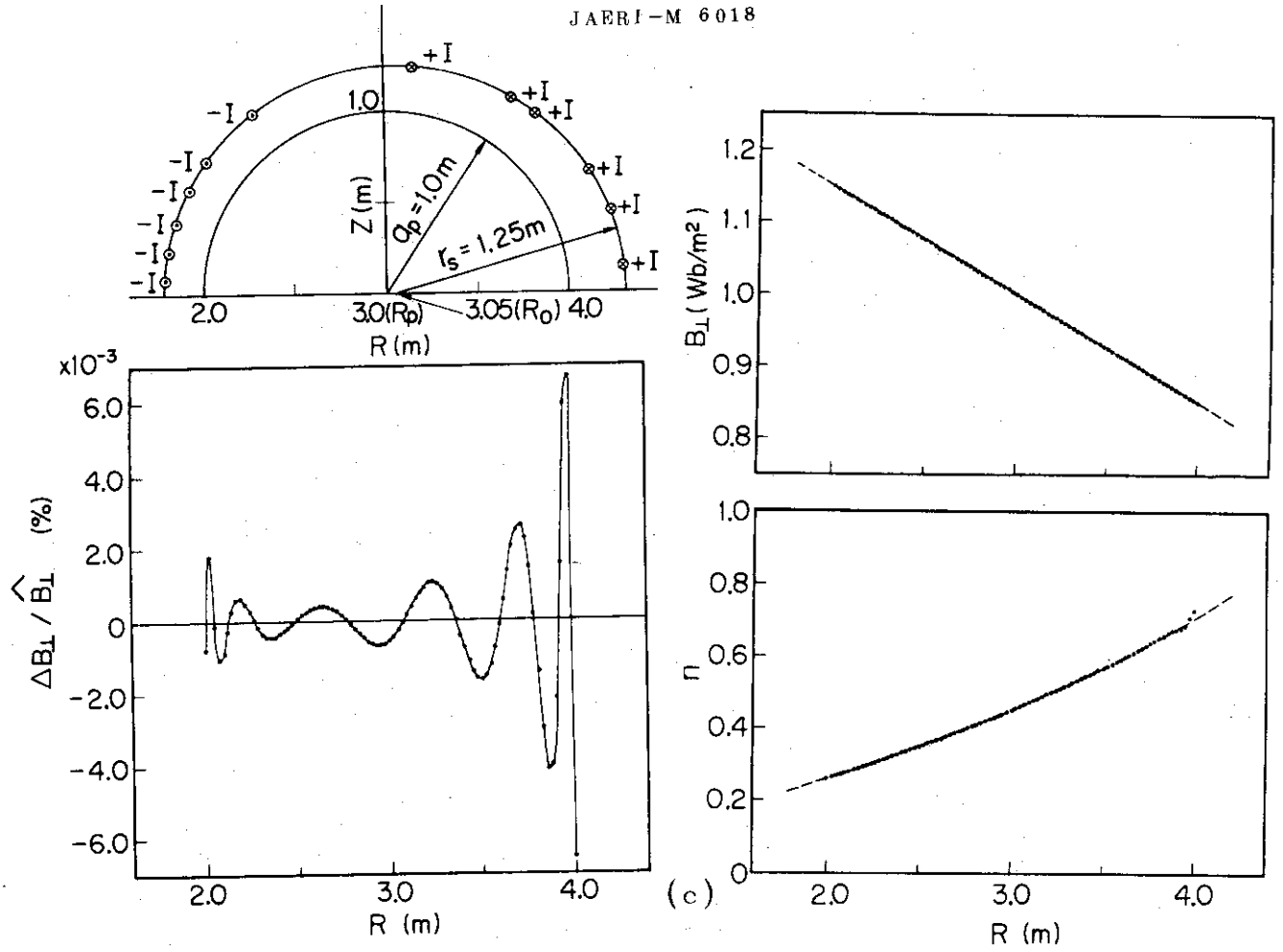
+I
-I
1.0
Z (m)
q_p=1.0m
r_s=1.25m
2.0
3.0(R_p)
3.05(R_0)
4.0
R (m)
x10^{-3}
$\Delta B_\perp / \hat{B}_\perp$ (%)
$B_\perp$ (Wb/m^2)
n
R (m)

(c)

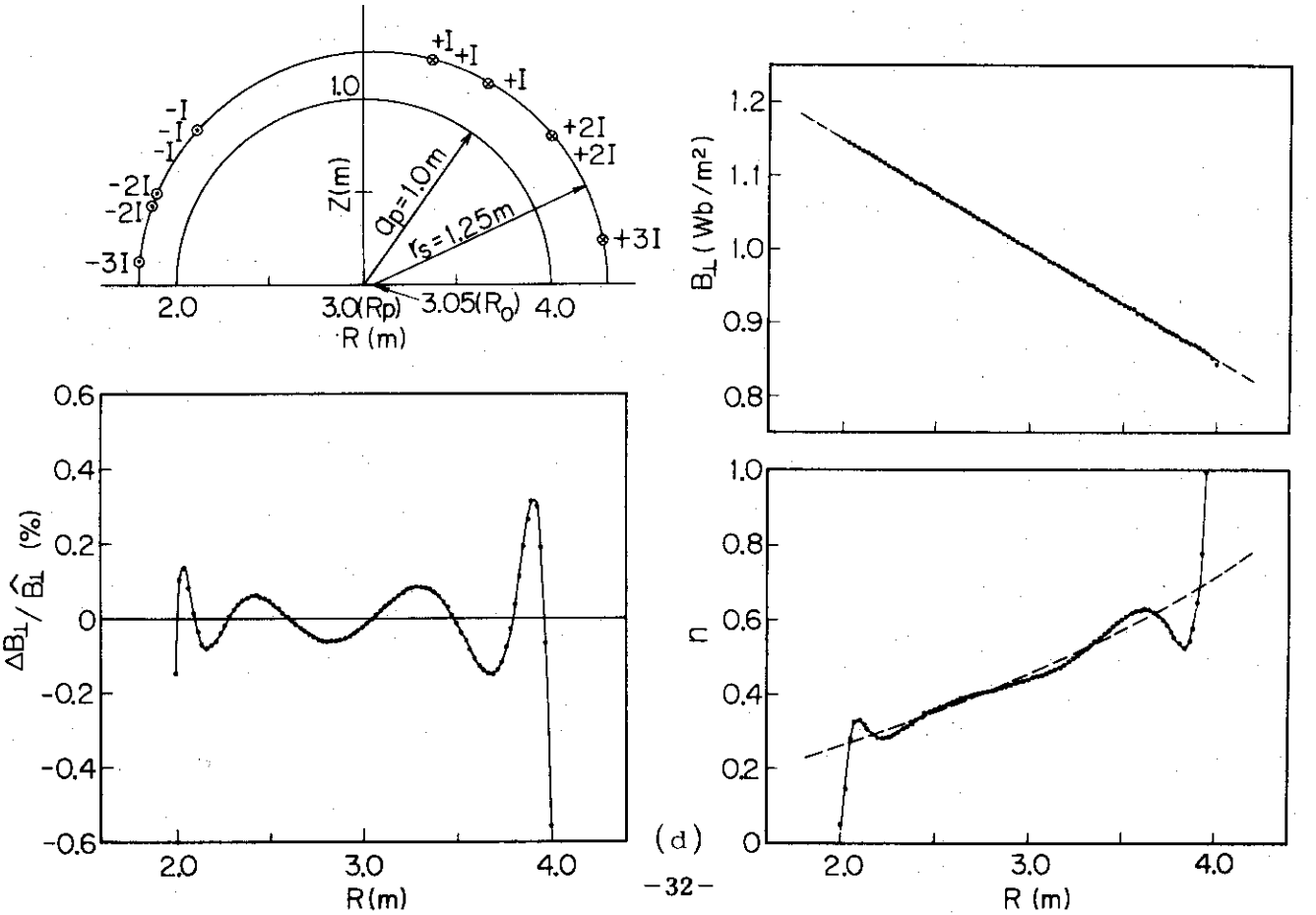
+I
-I
-2I
+2I
-3I
+3I
1.0
Z(m)
q_p=1.0m
r_s=1.25m
2.0
3.0(Rp)
3.05(R_0)
4.0
R (m)
$\Delta B_\perp / \hat{B}_\perp$ (%)
$B_\perp$ (Wb/m^2)
n
R (m)

(d)

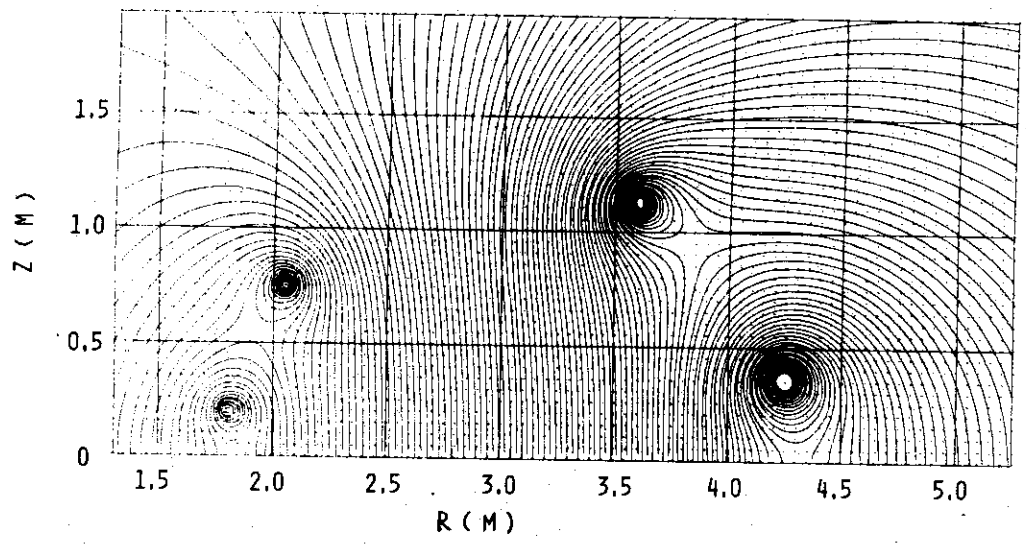
1.5
1.0
0.5
0
Z (M)
1.5
2.0
2.5
3.0
3.5
4.0
4.5
5.0
R (M)

(a)

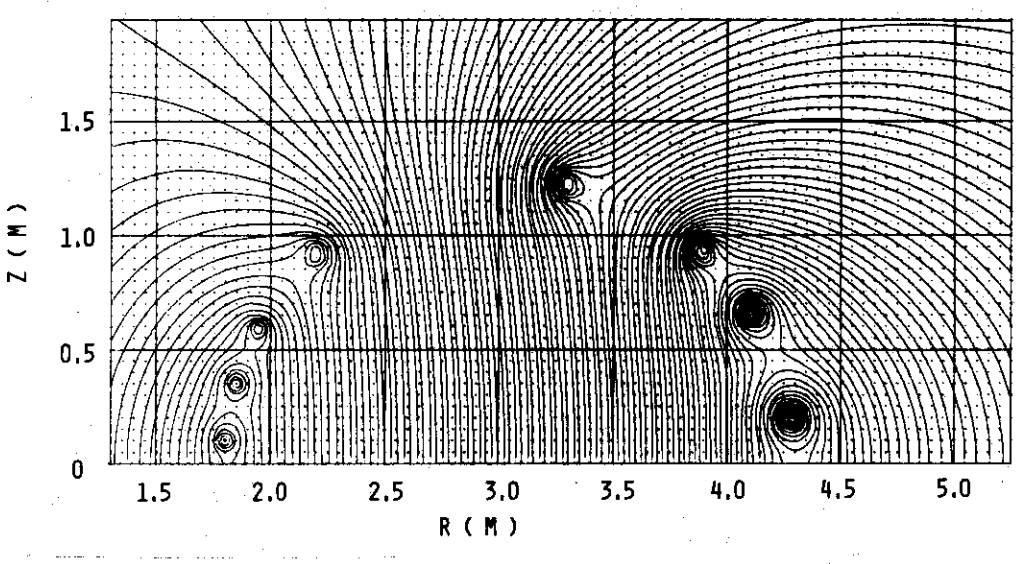
1.5
1.0
0.5
0
Z (M)
1.5
2.0
2.5
3.0
3.5
4.0
4.5
5.0
R (M)

(b)

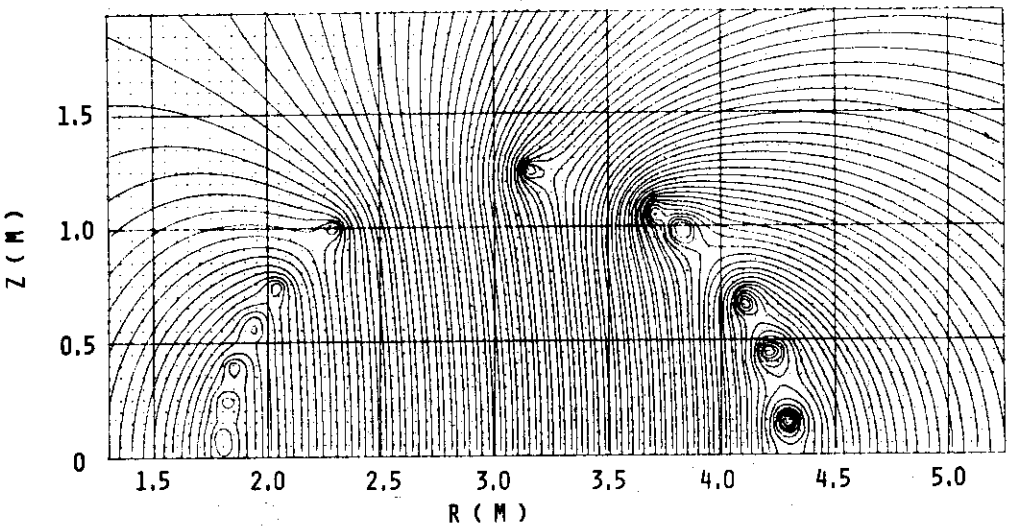

(c)

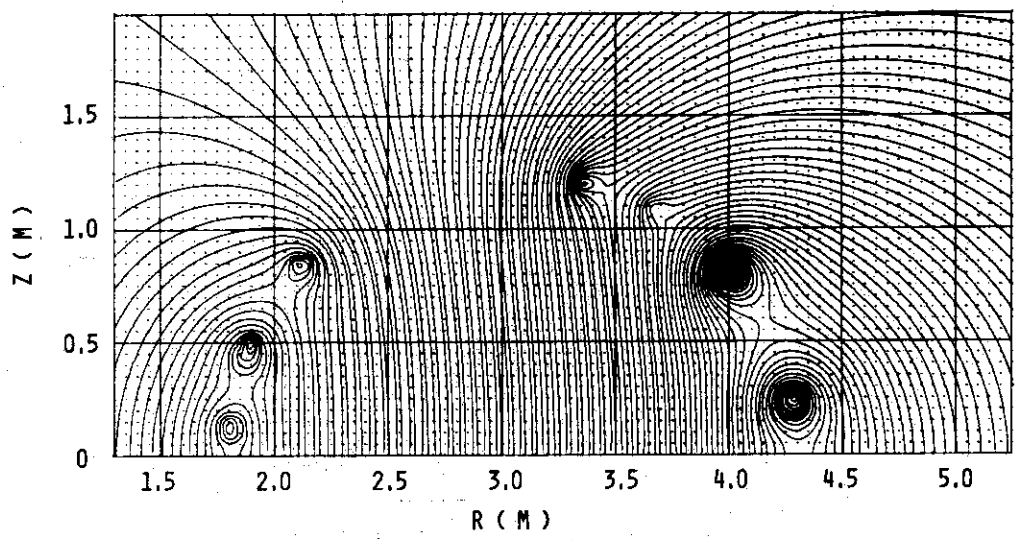

(d)

Fig.7. Two-dimensional patterns of the magnetic lines of force for the cases in Figs.6-(a), (b), (c) and (d).

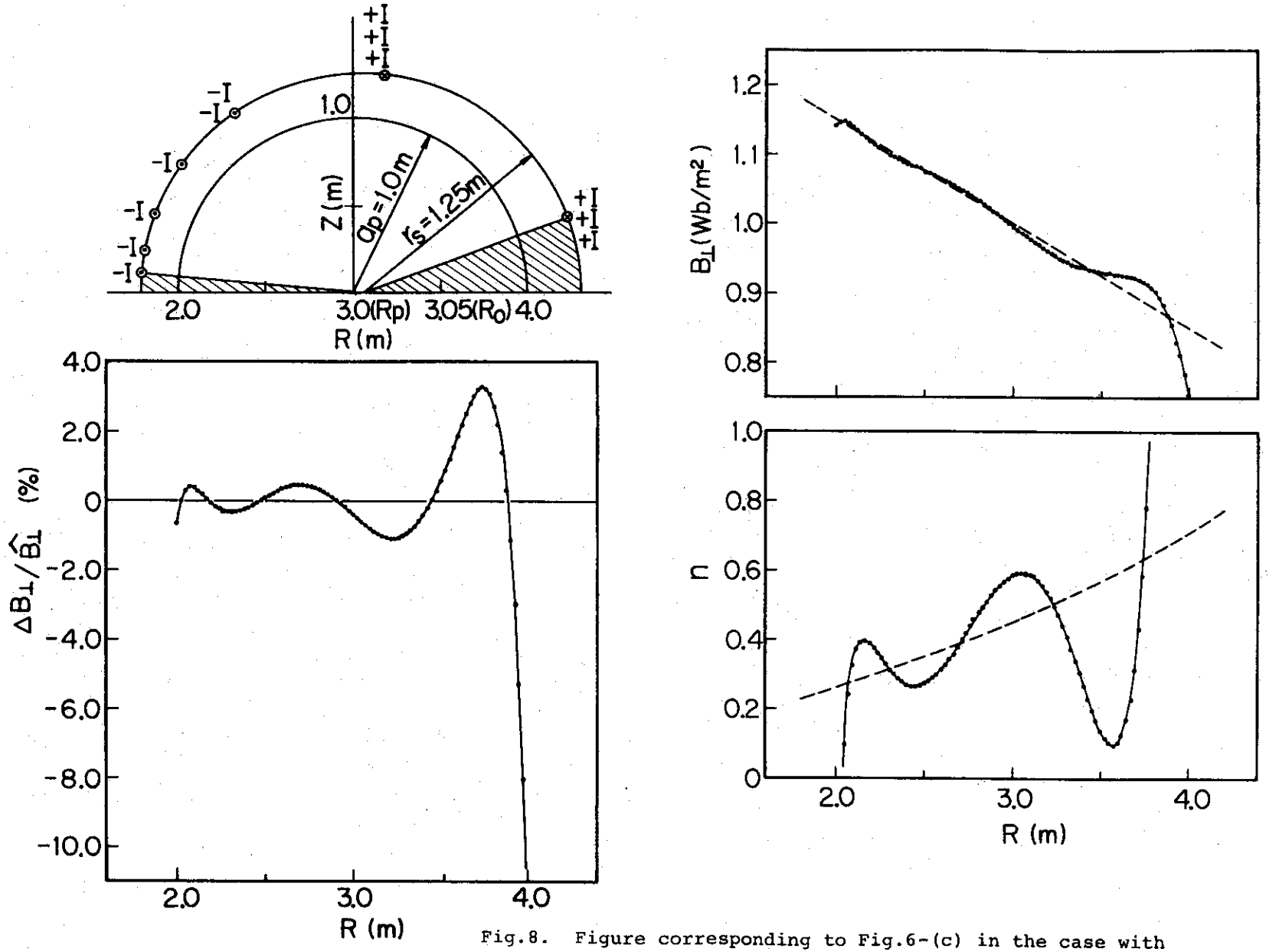

Fig.8. Figure corresponding to Fig.6-(c) in the case with the "forbidden region". The region is designated by the oblique lines. The substantial overlaps of several control loops appear.

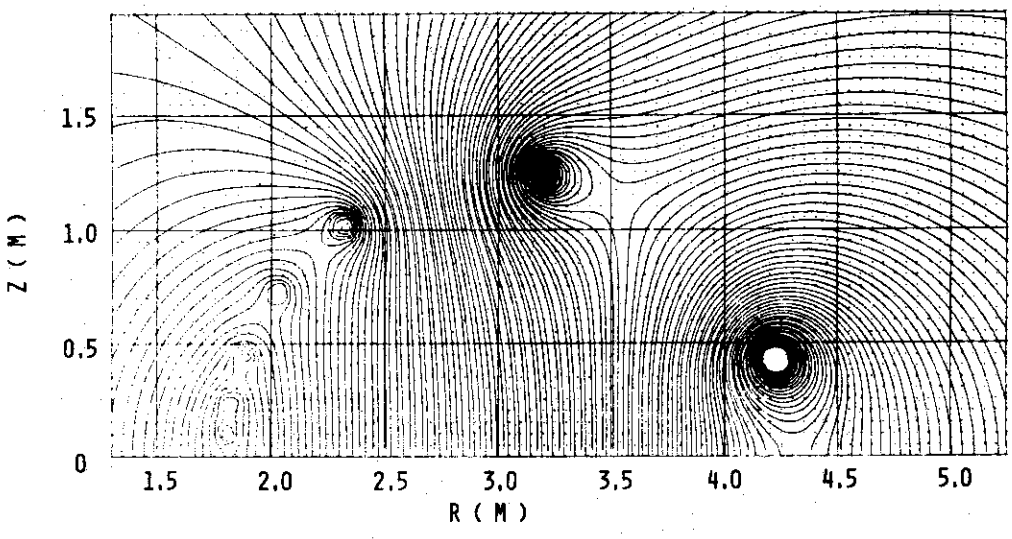

Fig.9. Two-dimensional pattern of the magnetic lines of force for the case in Fig.8.

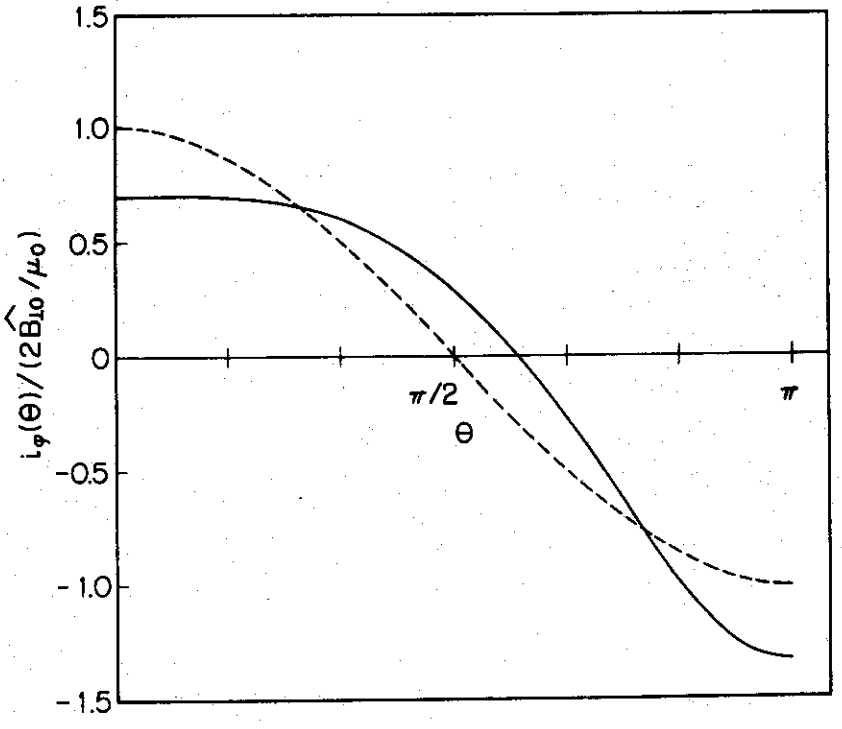

Fig.10. Poloidal distribution of the equivalent surface current density ($i_\varphi(\theta)$) to the current of the control loops by summing the Fourier components to the sixth harmonics. The broken and solid curves are the distributions for the cases shown in Figs.3 and 6-(c), respectively, where the former coincides with a cosine curve very well.

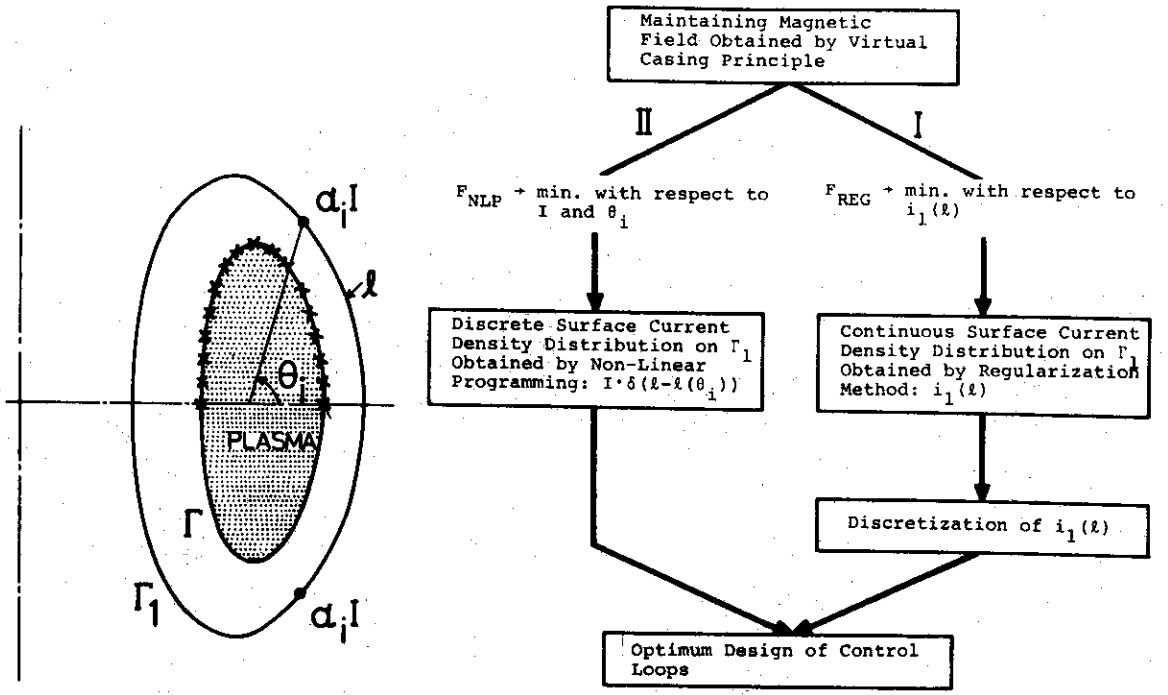

Fig.11. General procedure to obtain the optimum design of control loops. Lines I and II show the method in Ref.2 and the one based on the non-linear programming, respectively. The observation points of the magnetic field are shown on Γ by the crosses and F_{NLP} and F_{REG} are Eq.(1) in this article and the functional shown in section 3 of Ref.2, respectively.

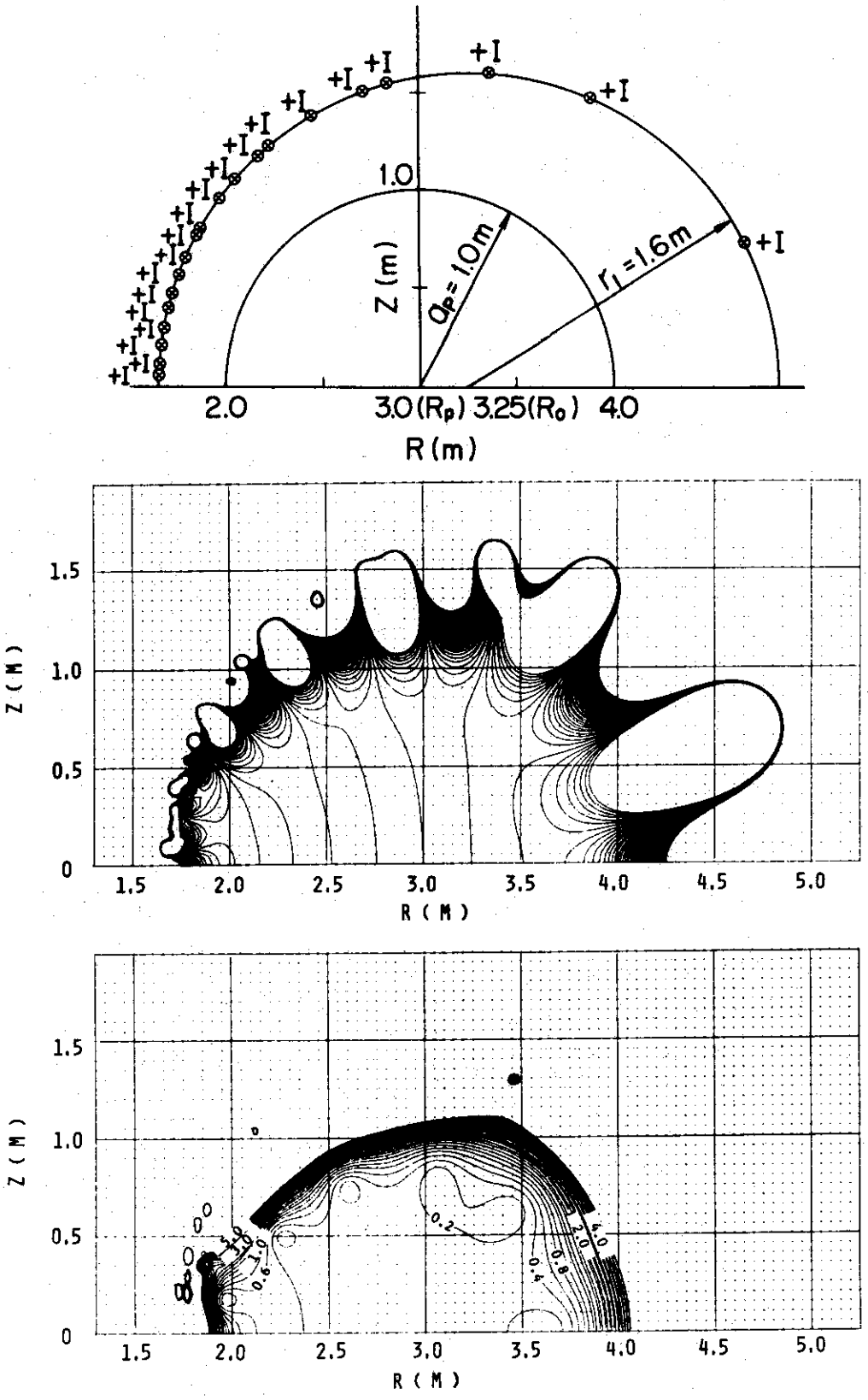

Fig.12. The optimum configuration of the primary windings (M = 20). The two-dimensional pattern of the magnetic lines of force and the magnitude of the magnetic field (gauss) for the total ampere-turn of 1 MAT.

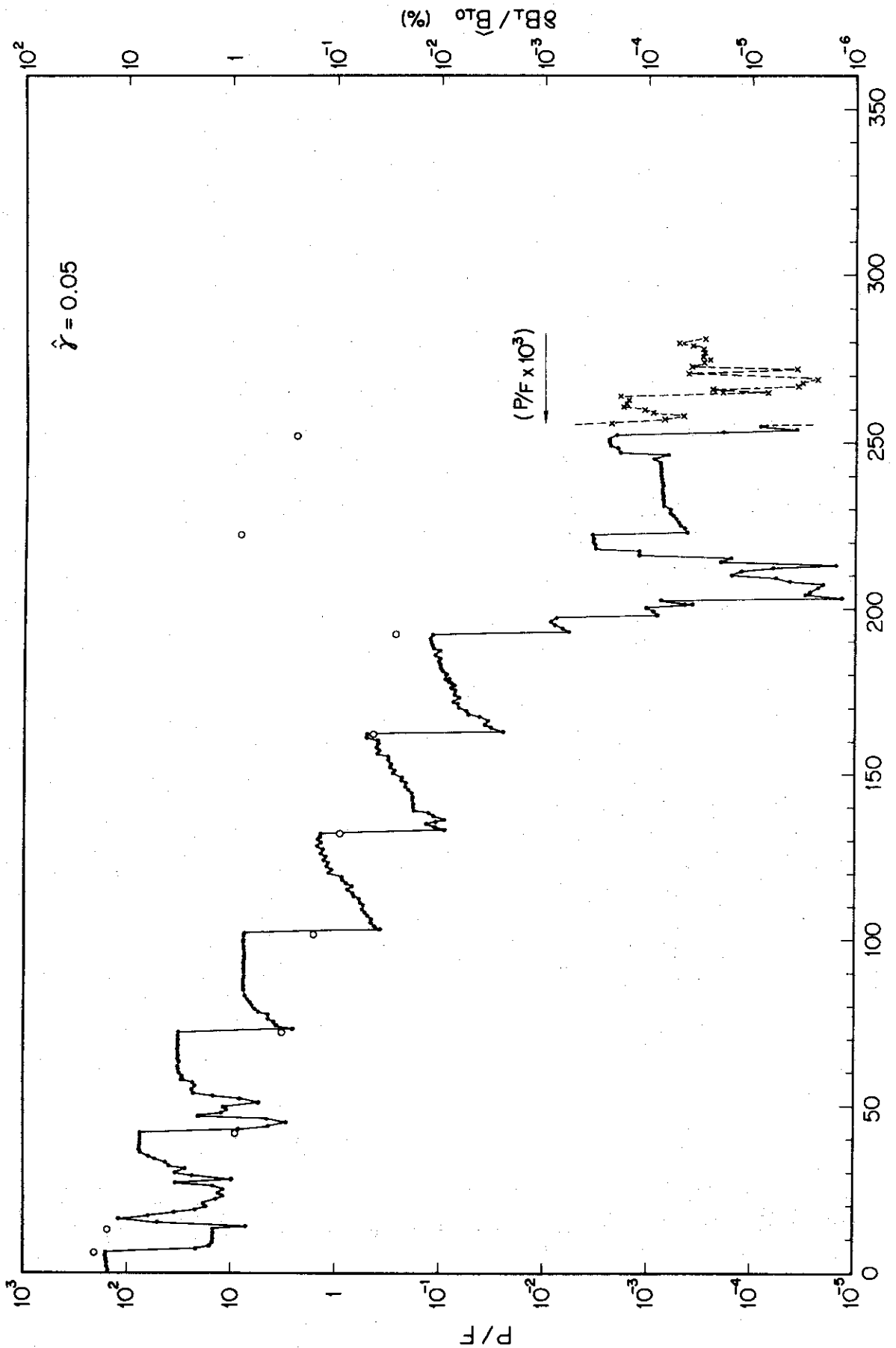
P/F
$\delta B_L / B_{L_0}$ (%)
$\hat{\gamma} = 0.05$
(P/F x 10^3)
0
50
100
150
200
250
300
350
10^3
10^2
10
1
10^{-1}
10^{-2}
10^{-3}
10^{-4}
10^{-5}
10^2
10
1
10^{-1}
10^{-2}
10^{-3}
10^{-4}
10^{-5}
10^{-6}

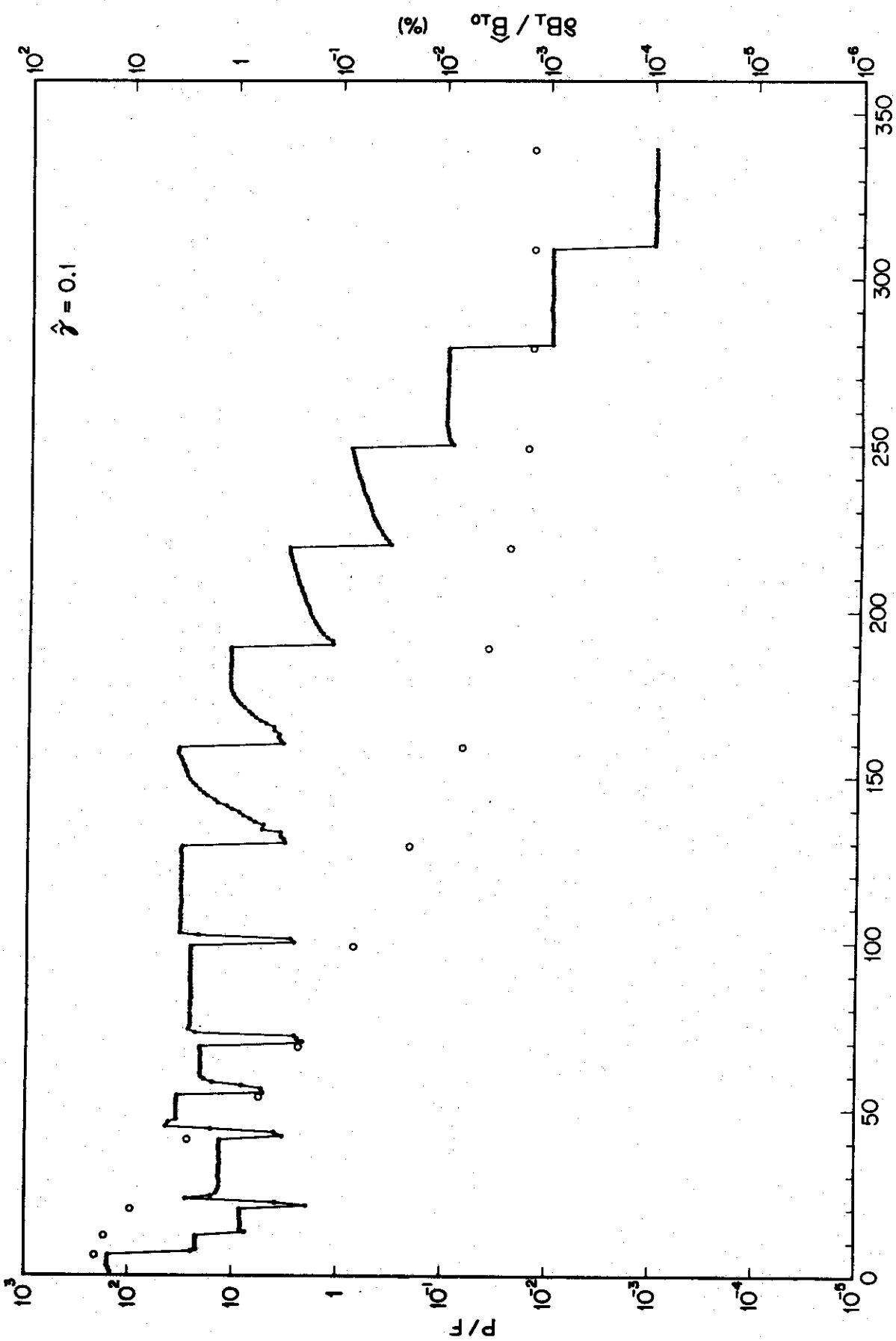

Fig.13. Behaviour of the ratio of the penalty function P to the original objective function F as a